

Investigation into Ultrasonic Testing of Thick Walled Austenitic Welds

Han T Y¹, Köhler B¹, Schmitz V², Zimmer A³, Langenberg K J³

(1. Fraunhofer IZFP-D, D-01109 Dresden, Germany; 2. Fraunhofer IZFP, D-66123 Saarbrücken, Germany;
3. Kassel University, 34121 Kassel, Germany)

Abstract: The ultrasonic testing (UT) of austenitic welds is difficult because they are not only anisotropic material in terms of elastic properties but heterogeneous material in terms of microstructure properties. The ultrasound wave in the austenitic weld is skewed along with crystallographic directions and scattered at weld boundaries. Since past decade, several tools for simulation of the wave propagation in highly anisotropic materials have been developed. In this paper, ray tracing and elastodynamic finite integration technique (EFIT) are applied to thick walled austenitic welds containing intergranular stress corrosion cracks (IGSCC) based on conventional UT method. It is demonstrated that the application of the ray tracing combined with EFIT shown in this paper can facilitate the selection of UT parameters.

Keywords: Austenitic weld; Ultrasonic testing; Elastodynamic finite integration technique (EFIT); Simulation; Crack

中图分类号: TG115.28 文献标志码: A 文章编号: 1000-6656(2009)11-0837-05

厚壁奥氏体焊缝超声波检测之探究

Han T Y¹, Köhler B¹, Schmitz V², Zimmer A³, Langenberg K J³

(1. 德国弗劳恩霍夫研究院 无损检测研究所(分部), 德累斯顿 D-01109, 德国; 2. 德国弗劳恩霍夫研究院 无损检测研究所, 萨尔布吕肯 D-66123, 德国; 3. 德国卡塞尔大学, 卡塞尔 34121, 德国)

摘要: 由于奥氏体焊缝中材料性能的各向异性和微观组织结构的不同, 奥氏体焊缝的超声波检测是非常困难的。超声波在奥氏体焊缝中会沿金属结晶方向发生偏转, 并在焊缝边界上发生散射。过去十年来, 人们开发了多种模拟各向异性材料中声波传播的仿真工具。本文则以常规超声波检测方法为基础, 将声线跟踪法和弹性动力学有限积分技术 (EFIT) 相结合, 应用于含晶间应力腐蚀裂纹的厚壁奥氏体焊缝中, 其结果显示声线跟踪法和弹性动力学有限积分技术 (EFIT) 结合应用, 有助于超声波检测参数的选取。

关键词: 奥氏体焊缝; 超声波检测; 弹性动力学有限积分技术; 仿真; 裂纹

It is difficult to obtain reliable results of ultrasonic testing to find flaws received from austenitic welds. Since anisotropic and inhomogeneous microstructures lead a direction dependent sound propagation concerning sound velocity, polarization, and mode conversion at interfaces, the phenomena involved are much more complex compared to testing of welds in ferritic steels. In the case of steels, i. e., isotropic and homogeneous microstructures, it is not a problem to define parameters for ultrasonic testing which is not the case for austenitic welds.

Numerical simulation tools can overcome the obstacles by comparing flaw indications for different

testing conditions and by selecting the most efficient ones. When taking a reliable ultrasonic testing for heterogeneous materials into consideration, it is desired to induce a straightforward simulation method. As one of the strongest simulation tools, the elastodynamic finite integration technique (EFIT) has been proposed by Langenberg, et al^[1-2].

Two different simulation tools are applied in this experiment. All of them are proved to be able to predict the sound propagation in elastically anisotropic and inhomogeneous welds^[3-4]. However, they have not yet been proved to be able to predict the indication of realistic flaws. Test specimens demonstrated in this

experiment were produced containing various types of austenitic weld cracks at different locations. The cracks are produced both by pure cycling and by a special method to initiate inter-granular stress corrosion cracking. In order to select optimized testing parameters, Ray tracing and EFIT simulation tools are applied to the weld geometry and to predetermined positions where cracks are expected to be found. Pulse-echo measurements of the flaw were carried out both with a specially designed probe and with conventional probes. It is turned out that the results of two simulations are well compliance with the predictions.

1 Fabrication of Welding Specimens^[5]

Austenitic welds have a key role in the pipe-jointing of the main structures of nuclear power plants. The austenitic steels used in nuclear power plants are X 8 CrNiTi 8 12, X 6 CrNi 18 11, X 10 CrNiTi 18 9, and X 10 CrNiNb 18 9. They do not differ essentially with respect to the dendritic structure of the welds. Therefore, no essential differences are expected in their elastic anisotropy. In this experiment, the test specimens were made of X 6 CrNi 18 11.

A U-groove weld with a base height of 2.5 mm, a radius of 6 mm, and a side wall angle of 9° was selected. The welds were built with manual arc welding. In order to make sure whether any other types of flaws which are not intended in the experiment exist or not, radiography was investigated and it was verified that there is no evidence of pores, inclusions, cracks or similar flaws. Additional liquid penetrant

testing was performed to characterise the cracks.

After welding, the whole plate was cut perpendicular to the weld to produce four pieces of specimens for the experiments. Additional edge-cuts of the plates at the weld ends were required to make a few pieces of small-sized samples for the metallographic investigations.

At the beginning, sharp notches were mechanically induced onto two specimens and then cracks started to grow under pure cycling loading. One crack started at the top layer and the other one was induced at the root of the weld. Intergranular stress corrosion cracks (IGSCC) were provoked on the third sample with special procedures. The IGSCC cracks started to generate at the weld root. As a reference, one specimen intentionally remains without any defect.

It is obviously shown from the microstructure investigation that significant dendrites are grown through several layers of the weld. It is observed that they are formed regularly (figure 1). Consequently, we can describe its' orientation analytically and apply it to radius model (figure 2).

The specimen, in which IGSCC cracks were induced, was thoroughly investigated. It is apparently shown that the IGSCC cracks lie in between the base and weld material along with heat affected zone (HAZ) (figure 2 and 3). The depth of the crack is about 10 mm. It was demonstrated with liquid penetrant testing that the crack is slightly wavy and reticulated.

The parameters input for the modelling were experimentally obtained. The each value obtained employing the base material is : sound velocities $c_L =$

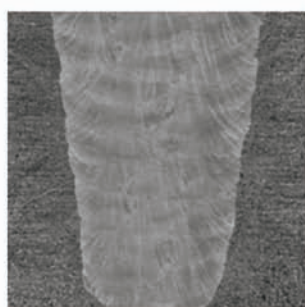


Fig. 1 Micrograph of the weld showing significant dendritic structure

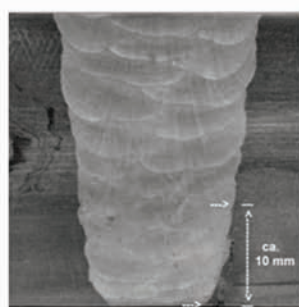


Fig. 2 Radius model of the dendrite orientation and its' distribution

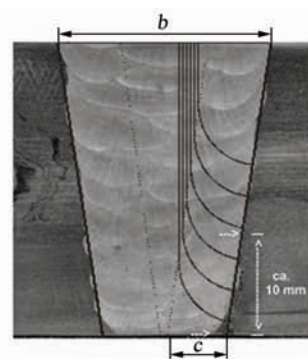


Fig. 3 Clipped side view of the specimen with IGSCC

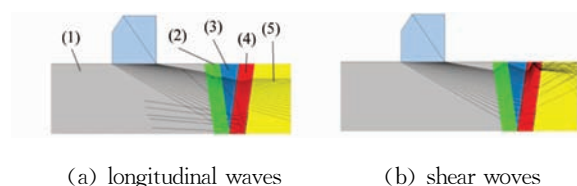
5.77 mm/ μ s, $c_T = 3.16$ mm/ μ s, and density $\rho = 7.88$ g/cm³, respectively. At the weld, the elastic constants^[3] $C_{11} = C_{22} = 263$ GPa, $C_{33} = 217$ GPa, $C_{13} = 145$ GPa, $C_{44} = 128$ GPa and $C_{66} = 82.4$ GPa were gained and the density was set equal to the value of the base material $\rho = 7.88$ g/cm³.

Due to the regular shape of the dendrites and analytical model, the radius model^[4], can be applied for description of their orientation and its' distribution. The dimension required for the modelling is: (a) inclination of the weld flank, the width of the weld at its root, (b) its top layer, and (c) the width of the region where the dendrites change their orientation in an arc shape fashion. According to the micrographs, each value is $a = (13.45 \pm 0.25)$ mm, $b = (22.75 \pm 0.25)$ mm, and $c = (6.75 \pm 0.15)$ mm, respectively.

2 Simulation of Ultrasound Wave Propagation and its Interaction with Cracks

2.1 Ray Tracing

Ray Tracing^[6] describes the wave propagation approximately in a bundle of ray. Each ray is followed along its energy propagation direction. At interfaces it can be chosen which wave mode is further considered. If ultrasound wave propagates into multiple interfaces as shown in figure 4 (Incident angle 70°. The wave mode is maintained in all layers. Layers: (1) grey - isotropic base material, (2) green - left zone of grain orientation change, (3) blue - core of the weld (grains are orientated parallel in thickness direction), (4) red - right zone of grain orientation change, (5) yellow - base material. There is a crack in 10 mm depth between red and yellow layer.), a large number of different variants will occur. Nevertheless, the wave propagation can be evaluated rapidly due to its' fast



(a) longitudinal waves (b) shear waves
Fig. 4 The result of ultrasound wave propagates into multiple interfaces

algorithm. The change in sound intensity resulted from divergence can be roughly estimated using the density of the beams.

The ray shown in the figure 4 propagates through all the boundaries and it maintains the original mode, i. e., (quasi-) longitudinal and (quasi-) shear vertically. It is clearly shown from the image that vertically polarized shear wave is strongly refracted at the interfaces and is deformed in the areas where the crystallite orientation varies. It was monitored that only a small amount of ray can reach the crack and it can hardly propagate back to the probe due to the scattering at the crack. Therefore, the process which is used to detect cracks and to evaluate them can be simplified provided that vertically polarized shear wave in all layers is eliminated.

As shown in figure 5, the propagation of the longitudinal wave is considered being converted at one of the interfaces into a vertically polarized shear wave. It becomes clear that a ray trace hitting the crack and travelling back to the probe is only possible with (quasi-) longitudinal waves in all layers. Considering these wave patterns, it can be concluded: the ultrasonic testing should be performed with longitudinal waves in the base material and with quasi longitudinal waves in the layers of the weld. The efficient incident angle is estimated when it is above 70°.

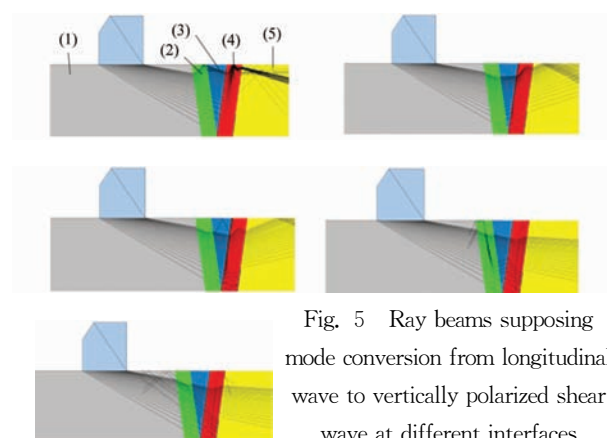


Fig. 5 Ray beams supposing mode conversion from longitudinal wave to vertically polarized shear wave at different interfaces

2.2 Elastodynamic Finite Integration Technique (EFIT)

The EFIT is a grid-based numerical time domain technique and easily treats different boundary conditions which are essential to model ultrasonic wave

propagation in heterogeneous materials.

The wave propagation for incident longitudinal waves was calculated for incident angles between 70° and 80° . The echo signals received from the crack were identified. The amplitudes of the signals increase when incident angles are over 70° , of which result approves itself the outcome of Ray tracing. In this experiment, it can be identified as shown in figure 6, in which five pieces of snapshots at selected time intervals of the wave propagation generating in 80° longitudinal wave mode are displayed. The various wave modes can be identified clearly. The ultrasound reflected at the crack travels back towards the probe, which facilitates signal interpretations (see arrow in figure 6). Correspondingly, the A-scan signals received through the simulation clearly represent the indication of the crack.

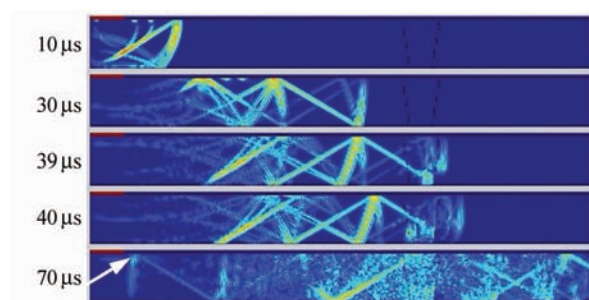


Fig. 6 Snapshots of the waves generated from a 80° longitudinal wave probe

The amplitude of the crack indication increases with higher incident angle and incident angles of 75° and 80° lead to approximately the same echo amplitudes.

3 Measurements to Verify Simulation

For the measurements to verify the result of the simulation, UT probes with broad bandwidth including wedges were used. Wedges for longitudinal waves were commercially available up to an incident angle of 70° . According to the fact resulted from the simulation that a higher possibility of crack detection is demonstrated when incident angles are over 70° , a specially designed wedge to meet this requirement was implemented by machining. To generate such a large incident angle, it is difficult to calculate the wedge angle in accordance with Snell's law^[7]. Therefore, the

wedge angle was determined by a probe optimisation program. The probe was finally characterised on a standard calibration block, K1, according to a conventional UT procedure^[8].

The measurements were successfully performed using EASYSCAN. The crack which is insonified by the longitudinal wave can be identified while the probe moves along a linear scan perpendicular to the weld. Several parallel scanning overlapping the paths was performed with offsets in weld direction.

It was hard to build both A-scan and B-scan images in this experiment. In the most preceded research focusing on detection of electronic discharge machining (EDM) notches in austenitic welds, it was not complicated to distinguish them from the grain noise at the weld. On the contrary, the amplitude of the echo from a natural crack is too small to distinguish from the other signals.

It was synthetic aperture focusing technique (SAFT) to show the crack clearly, in which seems to be related to the improvement of signal to noise ratio (figure 7). Further indications which are visible in the SAFT images are related to sound paths due to the contributions of quasi shear modes. Consequently, these indications can be located behind the crack when

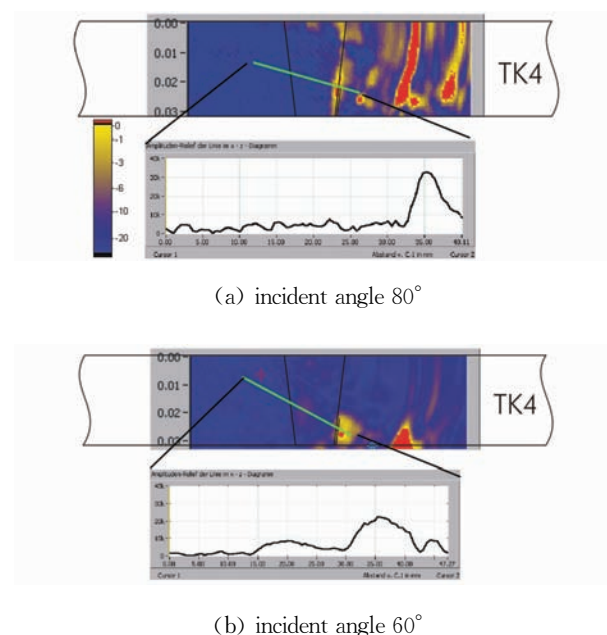


Fig. 7 SAFT-images overlaid to a scheme of the test body with indication of the position of the weld and the crack and amplitude changes along with the green line

it is considered at the probe side. They hardly produce difficulties with interpretation, however, when the probe on the weld is normally located.

The signal to noise ratio was determined to be 8, 14 and 16 dB for longitudinal wave incident at 60°, 70° and 80°, respectively. Thus, it is confirmed that the prediction of the simulations is well performed and incident angle higher than 70° yields good flaw indications.

4 Summary

Although it is challenging to simulate austenitic welds, we were fortunate to have the grain structures in the welds which turn out to be more stable. As a result, analytical model of the grain orientation and its' distribution can be applied. Ray tracing combined with EFIT simulation tool facilitates selection of optimal testing parameters in lab condition. It is demonstrated that SAFT betters the image quality and facilitates evaluation of the crack. It is well verified that the two tools combined can model the configuration of the heterogeneous anisotropic material.

As a future work, it is required to consider the noise generated during the simulation and to improve the signal to noise ratio.

References:

- [1] Fellingner P, Marklein R, Langenberg K J, et al. Numerical modeling of elastic wave propagation and scattering with EFIT - elastodynamic finite integration technique[J]. Wave Motion, 1995, 21(1): 47-66.
- [2] Langenberg K J, Hannemann R, Kaczorowski T, et al. Application of modeling techniques for ultrasonic austenitic weld inspection[J]. NDT & E International, 2000, 33(10): 465-480.
- [3] Walte F, Schurig C. Final report of the BMBF research project RS 1500931[R]. Saarbrücken, 1995.
- [4] Köhler B, Schurig Ch, Walte F, et al. Final report of the BMW research project RS 1501024[R]. Dresden, 2001.
- [5] Mletzko U. Report about fabrication of weld samples including grown cracks and grain structure analysis[R]. Staatliche Materialprüfungsanstalt (MPA), University Stuttgart, 2002.
- [6] Schmitz V, Walte F, Chakhlov S V. 3D-Ray Tracing in Austenite Materials[J]. NDT&E International, 1999, 32(4): 201-213.
- [7] Kühncke E. The limitations of Snell's law for the refraction of finite beams[J]. Wave Motion, 2002, 35(1): 1-15.
- [8] Köhler B, Schmitz V, Spies M, et al. Final report of the BMW research project No. 1501231 [R]. Dresden, 2004.



英国声纳检测集团
Sitiescan D10 / D20
超轻量便携式探伤仪

英国声纳的最新型号探伤仪一款, 此仪器特点是操作简易, 体积轻巧而坚固耐用, 能适合任何环境使用。

- 仪器重量仅 1.7 公斤(包括电池)
- 设计拥有防水 IP67 的国际标准
- 增益: 0-110dB, 步进: 0.5/1/2/6/10/14 和 20 dB
- 存储: 5000 幅 A 扫描波形, 100 组面板参考, 10,000 个测厚数据
- 输出: 线性模拟程控输出和复合视频 (PAL / NTSC)
- 支援中文操作界面
- 电池为 14.4v 锂电池, 常规使用可达 12 至 18 小时
- 可配功能: B 扫描, 闸门 2, DAC 功能(附加 DGS, AWS & API)

附件(可供选择件):

- 工具箱(含有各组件填装单元)
- 悬挂架
- 支撑、固定结构
- 背带
- 套索



产品质量 · 主导市场
Product Quality Leads Market